Journal of Control, Automation and Electrical Systems (2021) 32:42–56
https://doi.org/10.1007/s40313-020-00645-1

Periodic Event-Triggered Control for Linear Systems in the Presence of Cone-Bounded Nonlinear Inputs: A Discrete-Time Approach

G. B. Merlin[1] · L. G. Moreira[2] · J. M. Gomes da Silva Jr.[1]

Received: 2 March 2020 / Revised: 20 July 2020 / Accepted: 8 September 2020 / Published online: 9 November 2020

Abstract
This paper presents an observer-based periodic event-triggered strategy for linear systems subject to input cone-bounded nonlinearities. Considering a discrete-time framework, conditions in the form of linear matrix inequalities are derived to ensure global or regional stability of the origin of the closed-loop system under the event-triggered control strategy. These conditions are cast into convex optimization problems to determine the event-triggering function parameters, aiming at reducing the number of control updates with respect to periodic implementations. Both the emulation and the co-design problems are addressed. Numerical examples with logarithmic quantization and saturation nonlinearities are presented to illustrate the method.

Keywords Event-triggered control · Cone-bounded nonlinearities · Observers · LMIs · Co-design.

1 Introduction

Event-triggered control strategies have been attracting the attention of the control community in the last few years. The basic idea underlying these strategies regards updating the control signal only when a certain event, based on the measurement of states or outputs of the system, occurs (Heemels et al. 2012). The main motivation for the application of such a kind of updating control policy comes from the recently growth of the so-called networked control systems (NCS) (Hespanha et al. 2007), which brings some practical constraints in terms of the amount and the frequency of data transmissions. In this case, less control updates implies less amount and frequency of data transmissions. This has a clear impact, for instance, on network congestion and energy consumption (critical in systems fed by batteries). Another interesting motivation is to avoid actuators fatigue, which can be critical, for instance in mechanical devices.

Two basic problems can be formulated in the context of event-triggered control: the emulation and the co-design. In the emulation problem, the controller is supposed to be given and only the triggering function (or criterion) is designed. In the co-design, the controller and the triggering function are simultaneously synthesized.

Despite the fact that the majority of control systems nowadays are implemented digitally and, therefore, better modeled as discrete-time or sampled-data systems, most of the literature on event-triggered control considers a continuous-time setup, where the triggering function should be continuously evaluated (and then a continuous measurement of the state or outputs is assumed). Examples of this approach can be seen in Heemels et al. (2012), Selivanov and Fridman (2016), Abdelrahim et al. (2016), among many other references. Besides the unrealistic assumption of continuous measurements, from a theoretical point of view, the possibility of Zeno phenomenon is an extra concern. To overcome these issues, the idea is therefore to consider a periodic monitoring of the triggering function and a consequent periodic decision

This study was financed in part by CNPQ, Brazil (Grants PQ-305979/2019-9 and Univ-42299/2016-0) and IFSUL, Brazil (Project PD00190519/011).

✉ J. M. Gomes da Silva Jr.
jmgomes@ufrgs.br

G. B. Merlin
giovani.merlin@ufrgs.br

L. G. Moreira
lucianomoreira@charqueadas.ifsul.edu.br

[1] Departamento de Automação e Energia (DELAE), Universidade Federal do Rio Grande do Sul (UFRGS), Porto Alegre, Rio Grande do Sul, Brazil

[2] Instituto Federal de Educação, Ciência e Tecnologia Sul-rio-grandense (IFSul), Charqueadas, Rio Grande do Sul, Brazil

on updating or not the control signal. This is basically the idea proposed in Heemels et al. (2013), which was named *periodic event-triggered control* (PETC). Considering the same idea, but using exact discretization approaches (i.e., a discrete-time model) we can cite Eqtami et al. (2010), Braga et al. (2015), Hu et al. (2016) and Groff et al. (2016), which addresses observer-based feedback PETC for linear systems. More recently, Aranda-Escolástico et al. (2017) considered PETC with asynchronous transmissions of the output measurements and of the control inputs. In Wang et al. (2018), output-feedback PETC for nonlinear systems is addressed in an emulation context considering nonlinear controllers that stabilize the closed-loop system when implemented in a periodic (time-triggered) fashion. Cuenca et al. (2019) address PETC controllers for linear systems taking network delays and packet losses into account. PETC is also addressed, in the context of linear systems in Yue et al. (2013), Peng et al. (2013), Jia et al. (2014), Chen and Hao (2015), Zhang et al. (2015), Borgers et al. (2017), Oliveira et al. (2017), Linsenmayer et al. (2019), Liu and Yang (2019), Qi et al. (2020). Furthermore, considering generic nonlinear systems we can cite for instance Postoyan et al. (2013), Borgers et al. (2018), Yang et al. (2018), Wang et al. (2020). In particular, results obtained from the use of Takagi-Sugeno models can be found in Yan et al. (2019), Liu et al. (2020).

On the other hand, nonlinearities like saturation of actuators are ubiquitous in control systems. Moreover, in digital systems, quantization of controller output is also a subject of great interest. Many times, systems subject to these nonlinearities can be conveniently modeled as linear systems subject to sector-bounded input nonlinearities (see for instance Gomes da Silva and Tarbouriech 2005; Campos et al. 2018 and Moreira et al. 2016, which address event-triggered controllers for the specific case of these actuators nonlinearities). In Moreira et al. (2019), a method to design observer-based event-triggered controllers for this class of systems considering continuous monitoring of the system variables, i.e., a continuous-time ETC approach, is proposed.

The present work extends the results in Moreira et al. (2019) to consider the design of periodic observer-based PETCs for the class of nonlinear systems composed by a linear plant subject to cone-bounded (or sector-bounded) input nonlinearities. Here we also consider time-response performance requirements for the closed-loop system. This constraint is expressed as a minimum exponential decay rate requirement for the norm of the system states at sampling instants. Similarly to Groff et al. (2016), the problem is formulated in a discrete-time framework. Supposing that only the output of the plant is measurable, a discrete-time observer-based output feedback control law is considered. LMI-based conditions to ensure the closed-loop stability of the origin considering the event-triggered implementation, either in regional (i.e., local) as well as global contexts, are proposed. Both emulation and co-design problems are addressed. The stability conditions are then cast into convex optimization problems to compute the event-triggering function parameters aiming at a reduced number of control updates. In the case of co-design, the same objective is aimed, but considering the simultaneous synthesis of the event-triggering function parameters and the feedback gain matrix. Numerical examples are included to illustrate the application and potentialities of the method.

1.1 Notation

For a given matrix A, A' denotes its transpose. $A > 0$ means that A is positive definite. $\lambda_{\max}(A)$ and $\lambda_{\min}(A)$, the largest and the smallest eigenvalue of matrix A, respectively. $x[\cdot]$ denotes a discrete-time function. I and 0 are an identity matrix and a null matrix of appropriate dimensions. In partitioned matrices, $*$ stands for a symmetric block. $diag(A_1, ..., A_n)$ denotes a block diagonal matrix whose diagonal elements are the blocks A_1 through A_n.

2 Problem Statement

2.1 Problem Setup

Consider the following system, corresponding to the linear model of a plant whose control inputs are provided by a nonlinear actuator:

$$\begin{cases} \dot{x}_p(t) = A_p x_p(t) + B_p u(t) + B_{\text{pf}} f(u(t)) \\ y_p(t) = C_p x_p(t) \end{cases} \tag{1}$$

where $x_p \in \mathbb{R}^n$, $y_p \in \mathbb{R}^m$ and $u \in \mathbb{R}^p$ are the state, the output and the control signal, respectively. The matrices A_p, B_p, B_{pf} and C_p are supposed to be constant and of appropriate dimensions. Moreover, the function $f(u) : \mathbb{R}^p \to \mathbb{R}^p$ represents a known, decentralized cone-bounded nonlinearity affecting the input u. Therefore, it satisfies the following property:

$$f(u)'S(f(u) + Ju) \leq 0, \ \forall u \in \mathcal{S}_u \tag{2}$$

where $S \in \mathbb{R}^{p\times p}$ is any diagonal positive definite matrix and $J \in \mathbb{R}^{p\times p}$ is supposed to be a diagonal positive matrix that depends on the nonlinearity characteristics. Depending on the nonlinearity, condition (2) can be verified globally, i.e., $\forall u \in \mathbb{R}^p$, or only locally (regionally), i.e., $\forall u \in \mathcal{S}_u \subset \mathbb{R}^p$. In the regional case, we assume that $\mathcal{S}_u$ can be represented by a polytopic region as follows:

$$\mathcal{S}_u = \{u \in \mathbb{R}^p : |h_i'u| \leq 1; h_i \in \mathbb{R}^p, i = 1, ..., n_f\}. \tag{3}$$

Considering a digital control implementation, we suppose that the output of the system is sampled with a period T_s. Moreover, the control signal is supposed to be kept constant between two successive sampling instants by means of a zero-order hold, i.e., $u(kT_s+\tau) = u(kT_s),\ \forall\tau \in [0, T_s),\ \forall k \in \mathbb{N}$. From this setup, as the nonlinearity affects only the input, an exact discretization procedure leads to the following discrete-time model:

$$\begin{cases} x_p[k+1] = A_s x_p[k] + B_s u[k] + B_{\text{sf}} f(u[k]) \\ y_p[k] = C_s x_p[k] \end{cases} \tag{4}$$

with $x_p[k] = x_p(kT_s)$, $u[k] = u(kT_s)$, $A_s = e^{A_p T_s}$, $B_s = \int_0^{T_s} e^{A_p \tau} B_p d\tau$ and $B_{\text{sf}} = \int_0^{T_s} e^{A_p \tau} B_{\text{pf}} d\tau$.

We suppose that only the output of the plant y_p can be measured. Hence, to control the system we consider a discrete-time state observer, which is given by the following equations:

$$\begin{cases} x_o[k+1] = A_s x_o[k] + B_s u[k] + B_{\text{sf}} f(u[k]) - L e_y[k] \\ e_y[k] = y_p[k] - y_o[k] \\ y_o[k] = C_s x_o[k] \end{cases} \tag{5}$$

where $x_o \in \mathbb{R}^n$, $y_o \in \mathbb{R}^m$, $e_y \in \mathbb{R}^m$ are the observer state, the observer output and the output error, respectively. $L \in \mathbb{R}^{n\times m}$ is the observer gain matrix.

Considering now a classical digital observed state feedback control law, the control signal would be given by

$$u[k] = K x_o[k] \tag{6}$$

with $K \in \mathbb{R}^{p\times n}$ being the state feedback gain matrix. In this case, the control signal is supposed to be updated at each instant k from the estimated state at this instant. In what follows we refer to this strategy as a *periodic updating control* (PUC) strategy.

2.2 Event-Triggering Strategy

Differently from the periodic updating policy given by (6), the idea is to avoid unnecessary control updates by applying a *periodic event-triggered control* strategy (PETC), in the sense that at each sampling instant k, based on a trigger rule, a decision is made about updating the control signal or keeping it unchanged. Note that the *periodic* term in this case refers to the evaluation of the trigger rule periodically, at each instant k. More specifically, using a PETC strategy, the control signal is updated only at instants $k = n_i \in \mathbb{N}$, where n_i, $i = 1, 2, 3, \ldots$, denote the discrete-time instants in which a trigger is generated. In this case, the resulting control signal applied to the plant is described as follows:

$$u[k] = u[n_i] = K x_o[n_i], \quad \forall k \in [n_i, n_{i+1}). \tag{7}$$

Therefore, to provide a formulation for this implementation, we introduce the error vector between the value of the observed state at the last event instant and the current one, which is given by:

$$\delta[k] = x_o[n_i] - x_o[k], \tag{8}$$

From (8) and defining the observation error $e[k] = x_p[k] - x_o[k]$, the closed-loop system (4)–(5) can be re-written as follows:

$$\begin{cases} x_o[k+1] = (A_s + B_s K) x_o[k] + B_s K \delta[k] \\ \qquad\qquad + B_{\text{sf}} f(u[k]) - L C_s e[k] \\ e[k+1] = (A_s + L C_s) e[k] \end{cases} \tag{9}$$

which is equivalent to the compact form

$$x[k+1] = A x[k] + B\delta[k] + B_f f(u[k]) \tag{10}$$

with

$$A = \begin{bmatrix} A_s + B_s K & -L C_s \\ 0 & A_s + L C_s \end{bmatrix}, \quad B = \begin{bmatrix} B_s K \\ 0 \end{bmatrix},$$
$$B_f = \begin{bmatrix} B_{\text{sf}} \\ 0 \end{bmatrix}, \quad x[k] = \begin{bmatrix} x_o[k] \\ e[k] \end{bmatrix}.$$

The determination of the events instants, i.e., the event generation mechanism, is the key point of the ETC strategy. This is done through the evaluation of an appropriate triggering function $g(\delta[k], x[k])$. When g is positive, an event is triggered. In summary, the strategy consists in applying the following algorithm:

If $g(\delta[k], x[k]) > 0$ **then,**
$i = i + 1$
$n_i = k$
$u[n_i] = K x_o[k]$ (i.e., update the control signal)
else,
$u[k] = u[n_i]$ (i.e., keep the control signal)
end

In the present work, we will consider the triggering function given as follows Moreira et al. (2019):

$$g(\delta[k], x[k]) = \delta'[k] Q_\delta \delta[k] - \begin{bmatrix} x_o[k] \\ e_y[k] \end{bmatrix}' Q_\epsilon^{-1} \begin{bmatrix} x_o[k] \\ e_y[k] \end{bmatrix} \tag{11}$$

with $Q_\delta = Q_\delta' > 0 \in \mathbb{R}^{n\times n}$ and $Q_\epsilon = Q_\epsilon' > 0 \in \mathbb{R}^{(n+m)\times(n+m)}$. This choice is made to have the maximum possible degrees of freedom using only the available measurable signals (i.e., $x_o[k]$ and $e_y[k]$). The term $\delta'[k] Q_\delta \delta[k] - \begin{bmatrix} x_o[k] \\ e_y[k] \end{bmatrix}' Q_\epsilon^{-1} \begin{bmatrix} x_o[k] \\ e_y[k] \end{bmatrix}$ is a relative measure of the deviation between the value of the state/observer error at the last event

instant and the current one, including the output error. The matrices Q_δ and Q_ϵ act as weights on this measure. The triggering function (11) can therefore be seen as a generalization of the one proposed in Tabuada (2007).

2.3 Emulation and Co-design Problems

In this work, our aim is to reduce the number of control updates (i.e., the generation of events). Furthermore, we consider an exponential decay rate $0 < \alpha < 1$ for the norm of the system states at the sampling instants, that is, we aim at ensuring that

$$\|x[k]\| \leq \beta\alpha^k \|x[0]\|, \quad \forall k \in \mathbb{N}. \tag{12}$$

for some scalar $\beta > 0$.

Then, considering these specifications, we can formulate the emulation and co-design ETC design problems as follows:

- *Emulation Design:* considering a pre-computed observer-based control law that exponentially stabilizes the origin of the discrete-time closed-loop system (10) under periodic control updating, compute the triggering function parameters Q_δ and Q_ϵ to ensure the exponential stability of the origin of the discrete-time closed-loop system (10) under the event-triggering policy, while aiming at the reduction of the control updates with respect to the periodic control updating policy.
- *Co-design:* considering that only the observer gain is given, compute simultaneously the triggering function parameters and the state feedback gain to ensure the exponential stability of the origin of the discrete-time closed-loop system (10) under the event-triggering policy, aiming to reduce the number of control updates.

Depending on the validity of the sector condition (2), both problems can be addressed in a global or regional (local) context of stability. In the regional context, not all initial conditions lead to trajectories that converge to the origin. Therefore, in this case, it is fundamental to identify a region where convergence is ensured. Moreover, in many practical applications, it is important to ensure the convergence for all initial conditions in a given set $\mathcal{X}_0$ (i.e., a pre-specified set of admissible initial conditions) containing the origin.

3 Emulation Design

3.1 Stability Conditions

Given the controller gain K and the observer gain L, the following theorem provides LMI-based conditions for determining the matrices Q_ϵ and Q_δ of the triggering function (11) to ensure the exponential stability of the origin of system (10) in the regional case, i.e., if (2) is verified for $u \in \mathcal{S}_u$ with $\mathcal{S}_u$ as defined in (3).

Furthermore, it is also shown that the conditions ensure that the trajectories of the continuous plant (1) converge asymptotically to the origin. In particular, for a formal proof about that, the following assumption should be considered henceforth:

Assumption 1 If A_s has a pair of imaginary eigenvalues at $\pm j\omega_l$, the sampling period T_s is not an integer multiple of $\frac{2\pi}{w_l}$.

Note that this assumption is needed only to avoid a possible technical issue (as it will be seen in the proof of Theorem 1) and is not restrictive, as we can always chose an appropriate T_s that satisfies it.

Theorem 1 *If there exist symmetric positive definite matrices W, Q_δ, Q_ϵ, a diagonal positive definite matrix U, with appropriate dimensions, and a scalar η such that the following LMIs are verified:*

$$\begin{bmatrix} -\alpha^2 W & 0 & -(J\begin{bmatrix} K & 0 \end{bmatrix} W)' & (AW)' & (CW)' \\ * & -Q_\delta & -(JK)' & B' & 0 \\ * & * & -2U & (B_f U)' & 0 \\ * & * & * & -W & 0 \\ * & * & * & * & -Q_\epsilon \end{bmatrix} < 0 \tag{13}$$

$$\begin{bmatrix} W & W\begin{bmatrix} K' \\ 0 \end{bmatrix} h_i \\ * & \eta \end{bmatrix} > 0 \tag{14}$$

then provided that the initial condition $x[0] \in \mathcal{X} = \{x \in \mathbb{R}^{2n} : x'W^{-1}x \leq \eta^{-1}\}$ it follows that:

(a) *the state of the discrete-time closed-loop system (10), i.e., $x[k]$, converges to the origin as $k \to \infty$, with an exponential rate of at least α.*
(b) *the state of the continuous-time plant (1), i.e., $x_p(t)$, converges asymptotically to the origin as $t \to \infty$.*

Proof Consider the Lyapunov function candidate $V(x[k]) = x[k]'Px[k] > 0$, $P = P' > 0$. Defining $\Delta V(x[k]) = V(x[k+1]) - V(x[k])$ and omitting the dependency on k, we have:

$$\Delta V(x) = \Psi' N \Psi \tag{15}$$

with $\Psi = \begin{bmatrix} x' & \delta' & f' \end{bmatrix}'$, $M = \begin{bmatrix} A & B & B_f \end{bmatrix}$ and

$$N = \left(\begin{bmatrix} -P & 0 & 0 \\ 0 & 0 & 0 \\ 0 & 0 & 0 \end{bmatrix} + M'PM \right). \tag{16}$$

Recalling that $x = [x_o' \ e']'$ and $e_y = C_s e$, from the proposed ETC algorithm it follows that for $k \in (n_i, n_{i+1})$ one has:

$$g(\delta[k], x[k]) = \delta' Q_\delta \delta - x' C' Q_\epsilon^{-1} C x \leq 0 \tag{17}$$

where,

$$C = \begin{bmatrix} I & 0 \\ 0 & C_s \end{bmatrix}.$$

From the sector condition (2), we also have that the following relation is satisfied for all $u \in \mathcal{S}_u$:

$$2f'S(f + JK(x_o + \delta)) \leq 0. \tag{18}$$

On the other hand, considering an exponential decay rate $0 < \alpha < 1$, we have that $\|x[k]\| \leq \beta \alpha^k \|x[0]\|$ is satisfied if $V(x[k+1]) \leq \alpha^2 V(x[k])$. This requirement can thus be satisfied if:

$$\Delta V(x) < (\alpha^2 - 1)V(x) = (\alpha^2 - 1)x'Px. \tag{19}$$

Then, considering the S-Procedure with (17), (18) and (19) if

$$\begin{aligned} &\Psi' N \Psi - \delta' Q_\delta \delta + x' C' Q_\epsilon^{-1} C x - 2f'Sf \\ &\quad -2f'SJKx_o - 2f'SJK\delta - x'Px(\alpha^2 - 1) < 0 \end{aligned} \tag{20}$$

we have that (19) follows $\forall k \in (n_i, n_{i+1})$, provided that $u \in \mathcal{S}_u$. Rearranging the terms, we have that (20) is equivalent to

$$\Psi' \tilde{N} \Psi < 0 \tag{21}$$

with

$$\tilde{N} = \left(\begin{bmatrix} -\alpha^2 P + C' Q_\epsilon^{-1} C & 0 & -\left(SJ \begin{bmatrix} K & 0 \end{bmatrix}\right)' \\ 0 & -Q_\delta & -(SJK)' \\ -\left(SJ \begin{bmatrix} K & 0 \end{bmatrix}\right) & -(SJK) & -(S' + S) \end{bmatrix} + M'PM \right). \tag{22}$$

Hence, if $\tilde{N} < 0$ holds, then (19) is verified if $x \in \mathcal{S}_u$. Applying Schur's Complement to (22), pre- and post-multiplying the resulting matrix by $diag(W, I, U, I)$, with $W = P^{-1}$, $U = S^{-1}$ and finally applying Schur's Complement to the quadratic term $-W\alpha^2 + W'C' Q_\epsilon^{-1} CW$, it follows that $\tilde{N} < 0$ is equivalent to (13), which ensures that (19) holds. Consider now the triggering instant $k = n_i$. In this case $\delta[k]$ is set to zero and therefore $\tilde{N} < 0$ also ensures that (19) holds. Hence, if (13) is verified we conclude that $\Delta V(x) < (\alpha^2 - 1)V(x) < 0$, provided $u \in \mathcal{S}_u$.

We prove now that (14) guarantees $u[n_i] \in \mathcal{S}_u \ \forall n_i \geq 0$, whenever $x[0] \in \mathcal{X}$. Applying Schur's complement to (14) and then pre- and post-multiplying the result by $x[n_i]' W^{-1}$ and $W^{-1} x[n_i]$, respectively, one gets:

$$x[n_i]' \eta W^{-1} x[n_i] - u[n_i] h_i h_i' u[n_i] > 0, \tag{23}$$

Hence, if $x[n_i] \in \mathcal{X}$, it follows that $u[n_i] \in \mathcal{S}_u$. Consider now that $x[0] \in \mathcal{X}$. By definition $n_0 = 0$, and thus, we have that $u[n_0] = u[0] \in \mathcal{S}_u$, and from the satisfaction of (13), we conclude that $x[1] \in \mathcal{X}$. Note now that $u[1] = u[0]$ (if no trigger occurs at $k = 1$) or $u[1] = [K \ 0] x[1] = u[n_1]$ and in this case $u[1] \in \mathcal{S}_u$. Reapeating this reasoning for $k > 1$, we can therefore conclude that $u[k] \in \mathcal{S}_u$, $\forall k$. Hence, provided $x[0] \in \mathcal{X}$, we can conclude that (13) and (14) ensures that $\Delta V(x[k]) < 0$, $\forall k$, which concludes the proof of item a).

To prove item b), first notice that, from (1) and the triggering strategy, the dynamics of the continuous-time plant state $x_p(t)$ between two consecutive sampling instants, i.e., $\forall t \in [kT_s, (k+1)T_s)$ is given by:

$$\dot{x}_p(t) = A_p x_p(t) + B_p u(t_{n_i}) + B_{pf} f(u(t_{n_i})) \tag{24}$$

where $t_{n_i} = n_i T_s$ is the instant of the last control update event occurred before the current time t. Now let us define $t_k = kT_s$ and the elapsed time from the last sampling instant $\tau = t - t_k$. Considering these definitions, we can integrate (24) to compute:

$$\begin{aligned} x_p(t) = x_p(t_k + \tau) &= e^{A_p \tau} x_p(t_k) \\ &+ \int_0^\tau e^{A_p(\tau - s)} ds \left[B_p u_p(t_{n_i}) + B_{pf} f(u_p(t_{n_i})) \right] \end{aligned} \tag{25}$$

which is valid for all $t \in [t_k, \ t_{k+1})$, or, equivalently, for all $\tau \in [0, \ T_s)$.

From (25), it follows that

$$\begin{aligned} \|x_p(t)\| &\leq \|e^{A_p \tau}\| \|x_p(t_k)\| \\ &+ \left\| \int_0^\tau e^{A_p(\tau - s)} ds \right\| \left\| B_p u(t_{n_i}) + B_{pf} f(u_p(t_{n_i})) \right\| \end{aligned} \tag{26}$$

Since (2) ensures that $\|f(u)\| \leq \gamma_1 \|u\|$, $\forall u \in \mathcal{S}_u$ for some positive scalar γ_1 depending on J, we have:

$$\begin{aligned} \|x_p(t)\| &\leq \|e^{A_p \tau}\| \|x_p(t_k)\| \\ &+ \left\| \int_0^\tau e^{A_p(\tau - s)} ds \right\| \left(\|B_p\| + \gamma_1 \|B_{pf}\| \right) \|u(t_{n_i})\| \end{aligned} \tag{27}$$

On the other hand, from (7) we have:

$$\begin{aligned}\|u(t_{n_i})\| &= \|Kx_o[n_i]\| = \left\|\begin{bmatrix}K & 0\end{bmatrix}x[n_i]\right\| \\ &= \left\|\begin{bmatrix}K & 0\end{bmatrix}\right\| \|x[n_i]\|\end{aligned} \tag{28}$$

Thus, combining (27) and (28) and taking into account that $x_p(t_k) = \begin{bmatrix}I & I\end{bmatrix}x(t_k)$, we have that

$$\begin{aligned}\|x_p(t)\| \leq \|e^{A_p\tau}\| \left\|\begin{bmatrix}I & I\end{bmatrix}\right\| \|x[k]\| \\ + \left\|\int_0^\tau e^{A_p(\tau-s)}ds\right\| \gamma_2\|x[n_i]\|\end{aligned} \tag{29}$$

with $\gamma_2 = (\|B_p\| + \gamma_1\|B_{pf}\|)\left\|\begin{bmatrix}K & 0\end{bmatrix}\right\|$.

Observe now that the terms $e^{A_p\tau}$ and $\int_0^\tau e^{A_p(\tau-s)}ds$ depend only on τ and, since τ is bounded, they are bounded. Hence, there exist positive scalars γ_3 and γ_4 such that the following relation is valid for any $k \in \mathbb{N}$:

$$\|x_p(t)\| \leq \gamma_3\|x[k]\| + \gamma_4\|x[n_i]\|, \quad \forall t \in [t_k, t_{k+1}) \tag{30}$$

Hence, since from the proof of item a) $x[k] \to 0$ as $k \to \infty$, we can conclude that $x_p(t) \to 0$ as $t \to \infty$, provided that $n_i \to \infty$.

Suppose now that this is not the case, i.e., there exists $\bar{n}_i$ such that $u[k] = u[\bar{n}_i] = Kx_o[\bar{n}_i], \forall k \geq \bar{n}_i$. In this case, for $t \geq t_{\bar{n}_i} = \bar{n}_i T_s$ the plant evolution is given by the following equation:

$$\dot{x}_p(t) = A_p x_p(t) + \xi \tag{31}$$

with $\xi = B_p u(t_{\bar{n}_i}) + B_{pf} f(u(t_{\bar{n}_i}))$. Two situations arise:

(*i*) $\xi \neq 0$. In this case, system (31) will present an equilibrium point different from zero (in case A_p is singular we actually have a set of equilibria). Hence, if the initial state belongs to an invariant subspace defined by the eigenvectors (or generalized eigenvectors) associated to the eigenvalues of A_p with strictly negative real part, it follows that $x_p(t)$ will converge to this equilibrium point (which is different from the origin) as $t \to \infty$. Otherwise, $x_p(t)$ will either diverge or converge to a periodic orbit centered at the equilibrium point (which is different from the origin). In both cases, this represents a contradiction with the fact that $x[k] \to 0$ as $k \to \infty$, which implies that $x_p[k] \to 0$ as $k \to \infty$. Note that, in the case A_p has imaginary eigenvalues, the possibility of having the sampling instants coinciding with the possible crossing of the periodic orbit by zero is eliminated by Assumption 1.

(*ii*) $\xi = 0$. In this case, (30) reduces to

$$\|x_p(t)\| \leq \gamma_3 \left\|x_p(t_k)\right\|, \quad \forall t \in [t_k, t_{k+1}) \tag{32}$$

which, as $x[k] \to 0$ as $k \to \infty$, implies that $x_p(t) \to 0$ as $t \to \infty$.

Thus, from the two cases above one concludes that, in either case, $x_p(t)$ converges to the origin as $t \to \infty$, which ends the proof. □

Theorem 1 ensures that the origin of the discrete-time system (10) under the event-triggering strategy, with triggering function given by (11), is regionally exponentially stable with the set $\mathcal{X} = \{x \in \mathbb{R}^{2n} : x'W^{-1}x \leq \eta^{-1}\}$ included in its region of attraction. Moreover, it is ensured that the plant continuous-time trajectories converge asymptotically to the origin.

In the global case, i.e., when $\mathcal{S}_u = \mathbb{R}^p$, the following corollary can be formulated.

Corollary 1 *If there exist symmetric positive definite matrices W, Q_δ, Q_ϵ and a diagonal positive definite matrix U with appropriate dimensions such that LMI (13) is verified, then for all initial condition $x[0] \in \mathbb{R}^n$:*

(a) *the state of the discrete-time closed-loop system (10), i.e., $x[k]$, converges to the origin as $k \to \infty$, with an exponential rate of at least α.*
(b) *the state of the continuous-time plant (1), i.e., $x_p(t)$, converges asymptotically to the origin as $t \to \infty$.*

Proof The proof follows the steps of Theorem 1 without the use of constraint (14) since property (2) is supposed to be globally satisfied in this case. □

In this case, Corollary 1 ensures the global exponential stability of the origin of the discrete-time closed-loop system (10) and the global asymptotic stability of the continuous-time system (1), under the event-trigger strategy.

Remark 1 It should be noticed that if the conditions are verified with $\alpha = 1$, the exponential convergence of $x[k]$ is still ensured. In this case as the LMI (13) is strict, from the proof of Theorem 1 it follows that:

$$\Delta V(x) = \Psi' N \Psi < \Psi' \tilde{N} \Psi \leq -\epsilon||\Psi||^2 \leq -\epsilon||x||^2$$

with $\epsilon = |\lambda_{\max}(\tilde{N})|$. As there are positive scalars $\mu_2 = \lambda_{\max}(P)$ and $\mu_1 = \lambda_{min}(P)$ such that $\mu_1||x||^2 \leq V(x) \leq \mu_2||x||^2$, we can conclude that

$$\Delta V(x) < -\frac{\epsilon}{\mu_2} V(x)$$

and so it follows that $\Delta V(x) < (\tilde{\alpha} - 1)V(x)$ with $\tilde{\alpha} = (1 - \frac{\epsilon}{\mu_2})$. Note that, as $V(x[k+1]) > 0$, it follows that $0 < \tilde{\alpha} < 1$.

3.2 Optimization Problem

Conditions proposed in previous subsection ensure the asymptotic stability of the origin of the closed-loop system. In the present section, we cast these conditions into optimization problems as means to compute the triggering function parameters Q_δ and Q_e. For the regional case, we want to ensure that a given set $\mathcal{X}_0$ of admissible initial conditions is included in the region of attraction of the origin. This set can be defined as follows:

$$\mathcal{X}_0 = \{x \in \mathbb{R}^{2n} : x' P_0 x \leq 1\}, \tag{33}$$

where P_0 is a given symmetric positive definite matrix.

It is worth noticing that without this condition, the design can result in an arbitrarily small region of attraction, which is not useful in practice. Then, in order to compute the triggering function matrices, we propose the following optimization problem:

$$\begin{aligned} &\min \text{ trace } (Q_\delta) + \text{trace}(Q_\epsilon) \\ &\text{subject to : (13), (14), } W > \eta P_0^{-1}. \end{aligned} \tag{34}$$

The idea behind this optimization problem is to get the sum of the traces of Q_δ and Q_ϵ as small as possible, implying a maximization of the inter-event times with the trigger criterion (11). This occurs because the generation of an event happens only when the function g is positive. Hence, the negative term of the trigger criterion is maximized due to the minimization of trace(Q_ϵ) and the positive contribution, associated to Q_δ, is minimized. The constraint $W > \eta P_0^{-1}$ ensures that $\mathcal{X}_0 \subset \mathcal{X}$, guaranteeing that all trajectories initiating in $\mathcal{X}_0$ converge exponentially to the origin in discrete-time. For the global case, (34) without the constraints $W > \eta P_0^{-1}$ and (14) can be considered.

4 Co-design

4.1 Stability Conditions

Consider that the observer gain L is given, and define:

$$\tilde{A} = \begin{bmatrix} A_s & -LC_s \\ 0 & A_s + LC_s \end{bmatrix}, \quad \tilde{B} = \begin{bmatrix} B_s \\ 0 \end{bmatrix}.$$

The following theorem provides LMI-based conditions to simultaneously determine the matrices Q_ϵ and Q_δ of the triggering function (11) and the feedback gain K, to further reduce the triggering activity while ensuring the stability of the origin of the closed-loop system in the regional case.

Theorem 1 *th:Codesign If there exist symmetric positive definite matrices* $W = \left[\begin{smallmatrix} W_1 & 0 \\ 0 & W_2 \end{smallmatrix}\right]$, $Q_{\delta W}$, Q_ϵ, *a diagonal positive definite matrix* U, *a matrix* K_W, *with appropriate dimensions, and a scalar* η *such that the following LMIs are verified:*

$$\begin{bmatrix} -\alpha^2 W & 0 & -(J\begin{bmatrix} K_W & 0 \end{bmatrix})' & (\tilde{A}W + \tilde{B}\begin{bmatrix} K_W & 0 \end{bmatrix})' & (CW)' \\ * & -Q_{\delta W} & -(JK_W)' & (\tilde{B}K_W)' & 0 \\ * & * & -2U & (B_f U)' & 0 \\ * & * & * & -W & 0 \\ * & * & * & * & -Q_\epsilon \end{bmatrix} < 0 \tag{35}$$

$$\begin{bmatrix} W & \begin{bmatrix} K_W' \\ 0 \end{bmatrix} h_i \\ * & \eta \end{bmatrix} > 0 \tag{36}$$

then for $K = K_W W_1^{-1}$, $Q_\delta = W_1^{-1} Q_{\delta W} W_1^{-1}$ *and provided that the initial condition* $x[0] \in \mathcal{X} = \{x \in \mathbb{R}^{2n} : x' W^{-1} x \leq \eta^{-1}\}$ *it follows that:*

(a) *the state of the discrete-time closed-loop system (10), i.e.,* $x[k]$, *converges to the origin as* $k \to \infty$, *with an exponential rate of at least* α.
(b) *the state of the continuous-time plant (1), i.e.,* $x_p(t)$, *converges asymptotically to the origin as* $t \to \infty$.

Proof Noticing that $A = \tilde{A} + \tilde{B}\begin{bmatrix} K & 0 \end{bmatrix}$, and imposing the matrix structure $W = \left[\begin{smallmatrix} W_1 & 0 \\ 0 & W_2 \end{smallmatrix}\right]$, the proof basically follows analogous steps to the ones performed in the proof of Theorem 1. In particular, in this case, after applying Schur's Complement to $\tilde{N} < 0$, with $\tilde{N}$ defined in (22), we pre- and post-multiply the result by $diag(W, W_1, U, I)$ and consider the following variable changes to obtain (35):

$$K W_1 = K_W, \quad W_1 Q_\delta W_1 = Q_{\delta W}$$

Moreover, from these variable changes, it is straightforward to verify that (36) is equivalent to (14). □

In the case where $\mathcal{S}_u = \mathbb{R}^n$, the following corollary can be formulated:

Corollary 2 *If there exist symmetric positive definite matrices* $W = \left[\begin{smallmatrix} W_1 & 0 \\ 0 & W_2 \end{smallmatrix}\right]$, $Q_{\delta W}$, Q_ϵ, *a diagonal positive definite matrix* U *and a matrix* K_W, *with appropriate dimensions, such that LMI (35) is verified, then with* $K = K_W W_1^{-1}$ *and* $Q_\delta = W_1^{-1} Q_{\delta W} W_1^{-1}$ *it follows that for all initial condition* $x[0] \in \mathbb{R}^n$:

(a) *the state of the discrete-time closed-loop system (10), i.e.,* $x[k]$, *converges to the origin as* $k \to \infty$, *with an exponential rate of at least* α.
(b) *the state of the continuous-time plant (1), i.e.,* $x_p(t)$, *converges asymptotically to the origin as* $t \to \infty$.

Proof The proof follows the steps of Theorem 2 without the use of constraint (36) since property (2) is globally satisfied. □

4.2 Optimization Problem

In order to compute the triggering function matrices, Q_δ and Q_ϵ, and the controller gain K, aiming at reducing the number of control updates, we propose the following optimization problem:

$$\begin{aligned} &\min \ \ \text{trace}(Q_{\delta W}) + \text{trace}(Q_\epsilon) \\ &\text{subject to : (35), (36), } W > \eta P_0^{-1}. \end{aligned} \tag{37}$$

The motivation behind the optimization criterion in (37) is the same to (34). For the global case, (37) without the constraint $W > \eta P_0^{-1}$ and (36) can be considered.

Remark 2 The constraint imposed by the decay rate becomes more important for the co-design case. Since the objective is the number of control updates reduction, if one considers $\alpha = 1$, the resulting K can lead to a very slow closed-loop dynamics.

4.3 Re-design

It is worth noticing that the co-design approach employs conditions that are more conservative than the emulation design, by virtue of the structural constraint in the matrix W in Theorem 2. In this case, in order to get a further reduction on the generation of events it can be interesting to consider a re-design of the triggering function, for the computed gain K (Moreira et al. 2019). Thus the following two step procedure can be applied:

- Step 1: Compute the gain K from the optimization problem (37).
- Step 2: Solve the optimization problem (34) with the gain K obtained in step 1.

5 Numerical Examples

5.1 Example 1: Unstable Plant

Consider the unstable plant studied in Moreira et al. (2019):

$$\begin{cases} x_p(t) = \begin{bmatrix} 0 & 1 \\ 4 & 0 \end{bmatrix} x_p(t) + \begin{bmatrix} 0 \\ 1 \end{bmatrix} q(u(t)) \\ y(t) = \begin{bmatrix} 1 & 0 \end{bmatrix} x(t) \end{cases} \tag{38}$$

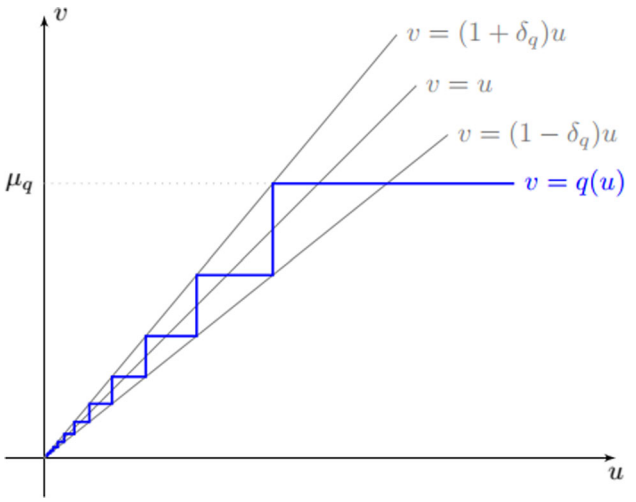

Fig. 1 Quantization function

Note that the plant in Example 1 could model the behavior of an inverted pendulum near the unstable equilibrium.

The function $q(u)$ corresponds to a logarithmic quantization of the control signal, being defined as follows:

$$q(u) = \begin{cases} \mu_q & if \ \ u \geq \frac{\mu_q}{1+\delta_q} \\ \rho_q^j \mu_q & if \ \ \frac{\rho_q^j \mu_q}{1+\delta_q} \leq u < \frac{\rho_q^j \mu_q}{1-\delta_q}, \ j \in \{1, 2, ...\} \\ 0 & if \ \ u = 0 \\ -\rho_q^j \mu_q & if \ \ -\frac{\rho_q^j \mu_q}{1+\delta_q} \geq u > -\frac{\rho_q^j \mu_q}{1-\delta_q}, \ j \in \{1, 2, ...\} \\ -\mu_q & if \ \ u \leq -\frac{\mu_q}{1+\delta_q} \end{cases} \tag{39}$$

with the quantization parameters

$$0 < \rho_q < 1, \qquad \delta_q = \frac{1-\rho_q}{1+\rho_q}, \qquad \mu_q > 0,$$

where ρ_q is the density of quantization and μ_q the maximum level of quantization (Campos et al. 2018). The positive branch of $q(u)$ is depicted in Fig. 1.

Considering the quantization error $\hat{q} = q(u) - u$, it follows that $\hat{q}$ is sector-bounded by $\pm\delta_q u$. Hence, making the change of variables $f(u) = \hat{q} - \delta_q u$, results that $f(u)(f(u) + 2\delta_q u) \leq 0$, i.e., condition (2) is satisfied with $J = 2\delta_q$ if $|u| \leq \frac{\mu_q}{1-\delta_q}$ or, equivalently, if $|\frac{1-\delta_q}{\mu_q} u| \leq 1$.

For a sampling period of $T_s = 0.02$, the discrete-time system (4) is obtained with:

$$A_s = \begin{bmatrix} 1.001 & 0.02001 \\ 0.08002 & 1.001 \end{bmatrix}, \quad B_s = \begin{bmatrix} 0.0002106 \\ 0.02106 \end{bmatrix},$$
$$B_{sf} = \begin{bmatrix} 0.0002 \\ 0.02001 \end{bmatrix}, \quad C_s = \begin{bmatrix} 1 & 0 \end{bmatrix}.$$

In this example, the considered quantization parameters are $\rho_q = 0.9$ and $\mu_q = 35$, which results in $\delta_q \approx 0.05263$.

Emulation case

For the emulation case, we consider the observer gain $L = \begin{bmatrix}-0.07 & -0.14\end{bmatrix}'$, the controller gain $K = \begin{bmatrix}-36.89 & -11.96\end{bmatrix}$ and $\mathcal{X}_0$ as defined in (33), with $P_0 = diag(10^6, 10^6, 0.5, 0.1)$. In this case, we do not specify a decay rate α restriction, i.e., we consider $\alpha = 1$ in the conditions (which ensures only that $\Delta V(x) < 0$). Considering that the sector condition is valid only if $|\frac{1-\delta_q}{\mu_q}u| \leq 1$, it follows that $\mathcal{S}_u = \{u \in \mathbb{R} : |0.0271u| \leq 1\}$. Then, solving the optimization problem (34) yields the following triggering function parameters:

$$Q_\delta = \begin{bmatrix}14.91 & 4.831\\ 4.831 & 1.57\end{bmatrix}, \quad Q_\epsilon = \begin{bmatrix}2.329 & -3.65 & 2.026\\ -3.65 & 10.82 & -1.209\\ 2.026 & -1.209 & 3.379\end{bmatrix}.$$

Simulating the closed-loop system with the designed PETC, considering $x_o[0] = [0 \quad 0]'$ and $x_p[0] = [-1 \quad 1.5]'$, and comparing to a standard periodic updating control strategy (PUC) (i.e., the control signal is updated in all sampling instants), the responses obtained for the plant states (x_p) and the control signal are shown in Fig. 2. The bottom plot shows the event times. The size of the bars depicts the inter-event times, i.e., the number of instants k between that event and the previous one. It can be noticed that the event-trigger policy has efficiently reduced the number of control updates with respect to the periodic strategy while assuring approximately the same response. On the interval $0 < k \leq 350$, the control has been updated 42 times in the PETC strategy, versus 350 times in the standard PUC strategy.

Co-design case

For the co-design case, we consider the same parameters $L = [-0.07 \quad -0.14]'$ and $P_0 = diag(10^6, 10^6, 0.5, 0.1)$, $\alpha = 1$, leading to the following solution to optimization problem (37):

$$Q_\delta = \begin{bmatrix}7.74 \cdot 10^{13} & 2.429 \cdot 10^{13}\\ 2.429 \cdot 10^{13} & 8.477 \cdot 10^{12}\end{bmatrix},$$

$$Q_\epsilon = \begin{bmatrix}1.74 \cdot 10^{-11} & -1.33 \cdot 10^{-11} & 5.208 \cdot 10^{-12}\\ -1.33 \cdot 10^{-11} & 3.175 \cdot 10^{-11} & -1.202 \cdot 10^{-12}\\ 5.208 \cdot 10^{-12} & -1.202 \cdot 10^{-12} & 1.026 \cdot 10^{-11}\end{bmatrix},$$

$$K = \begin{bmatrix}-15.52 & -6.681\end{bmatrix}.$$

With the same initial conditions of the emulation case, the simulation of the closed-loop system obtained for the co-design is shown in Fig. 3. The same observations done for the emulation case can be made. The control, however, is updated 119 times versus 42 times in the emulation case, i.e., the simultaneous design of the gain and the triggering strategy provided no improvement with respect to the emulation case. As commented in Sect. 4.3, this basically comes from the fact

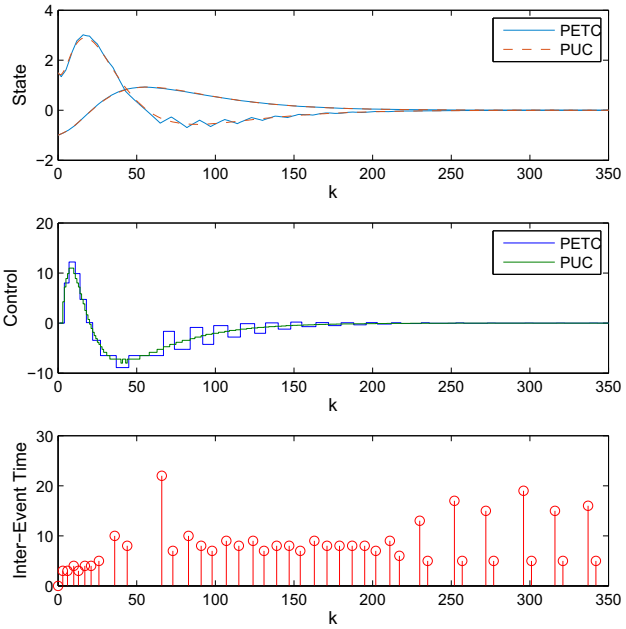

Fig. 2 Example 1: response with the PETC obtained from emulation and with the standard PUC strategy

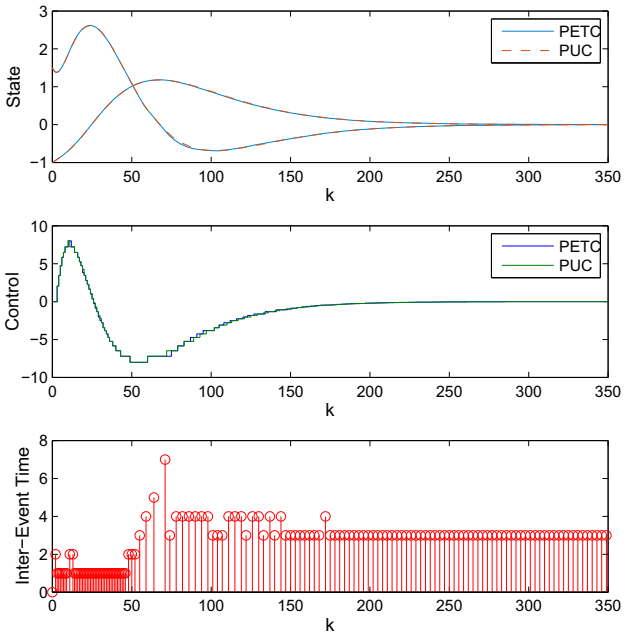

Fig. 3 Example 1: response with the PETC obtained from the co-design and with the standard PUC strategy

that the co-design approach employs conditions that are more conservative, in the sense that a block diagonal structure in the matrix W is imposed.

We still can apply a redesign procedure as discussed in Sect. 4.3, i.e., considering the computed gain matrix K, we solve problem (34) to refine matrices Q_ϵ and Q_δ in order to

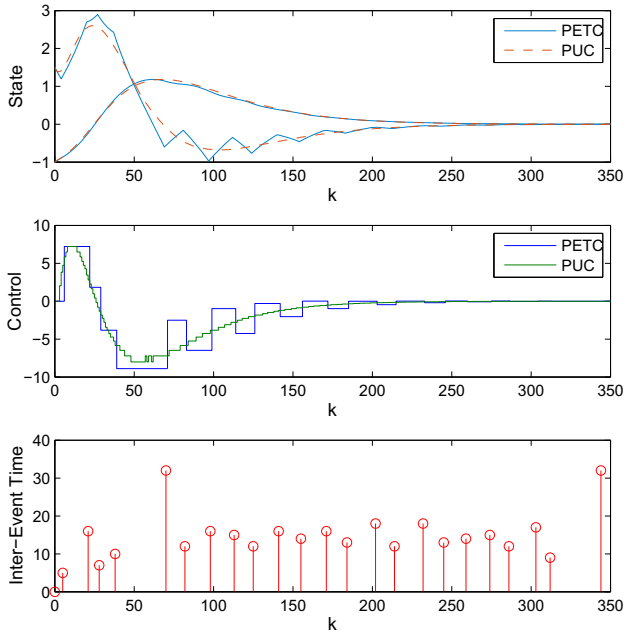

Fig. 4 Example 1: response with the PETC obtained from re-design and with the standard PUC strategy

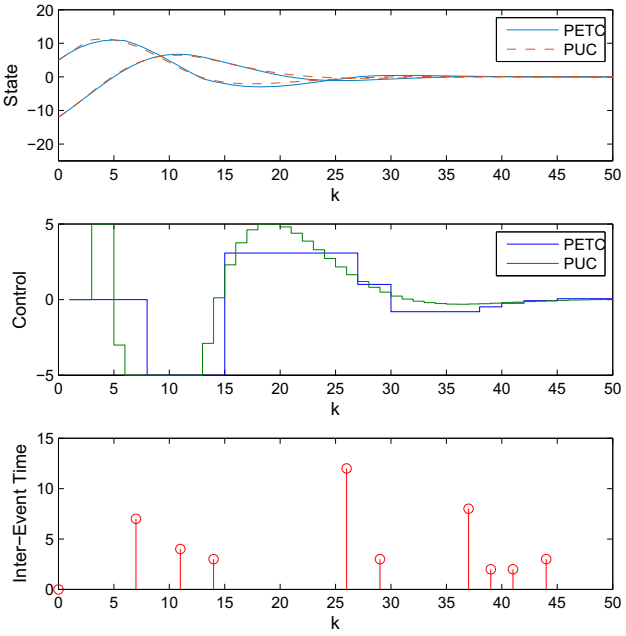

Fig. 5 Example 2: response with the PETC obtained from emulation and with the standard PUC strategy

reduce the number of control updates. This procedure leads to:

$$Q_\delta = \begin{bmatrix} 5.41 & 2.329 \\ 2.329 & 1.003 \end{bmatrix},$$

$$Q_\epsilon = \begin{bmatrix} 2.212 & -1.224 & 0.8566 \\ -1.224 & 3.602 & -0.03111 \\ 0.8566 & -0.03111 & 0.6068 \end{bmatrix}.$$

Simulating with the same initial conditions of the previous cases, the response of the closed-loop system generated from the re-design parameters is shown in Fig. 4. It can be observed that the re-design procedure leads to a significant reduction in the number of control updates, resulting in only 24.

5.2 Example 2: Global Stabilization

Now we consider the following stable plant:

$$\begin{cases} \dot{x}_p(t) = \begin{bmatrix} -1 & 2 \\ -2 & 0 \end{bmatrix} x_p(t) + \begin{bmatrix} 0 \\ 1 \end{bmatrix} sat(u(t)) \\ y(t) = \begin{bmatrix} 1 & 0 \end{bmatrix} x(t) \end{cases} \tag{40}$$

where $sat(u(t))$ is a saturation function of the actuator with saturation levels ± 5. The corresponding discrete-time version of (40) with a sampling period $T_s = 0.1$ is given by:

$$\begin{cases} x_p[k+1] = \begin{bmatrix} 0.8862 & 0.1891 \\ -0.1891 & 0.9807 \end{bmatrix} x_p[k] + \begin{bmatrix} 0.009643 \\ 0.09935 \end{bmatrix} sat(u[k]) \\ y[k] = \begin{bmatrix} 1 & 0 \end{bmatrix} x[k] \end{cases} \tag{41}$$

Considering the dead-zone function $f(u) = sat(u) - u$, system (41) can be re-written in the form (10), while satisfying the condition (2) with $J = 1$ globally, i.e., $\forall u \in \mathbb{R}$. Furthermore, this change implies $B_{sf} = B_s$.

Emulation Case

Consider the emulation problem with the control gain $K = \begin{bmatrix} 0.33 & -2 \end{bmatrix}$ and the observer gain $L = \begin{bmatrix} -1.16 & -1.91 \end{bmatrix}'$. Applying the optimization problem (34) for the global case, with a decay rate $\alpha = 0.98$ and an additional constraint $\lambda_{\max}(Q_\epsilon) < 10^4 \lambda_{min}(Q_\epsilon)$ (to avoid ill conditioned solutions), leads to the following matrices for the triggering function (11):

$$Q_\delta = \begin{bmatrix} 0.06156 & -0.3703 \\ -0.3703 & 2.245 \end{bmatrix},$$

$$Q_\epsilon = \begin{bmatrix} 1.004 & 0.1805 & 6.004 \cdot 10^{-5} \\ 0.1805 & 1.303 & -9.036 \cdot 10^{-6} \\ 6.004 \cdot 10^{-5} & -9.036 \cdot 10^{-6} & 0.002018 \end{bmatrix}.$$

Performing a simulation of the closed-loop system with the designed PETC and with the PUC strategy, considering $x_o[0] = \begin{bmatrix} 0 & 0 \end{bmatrix}'$ and $x_p[0] = \begin{bmatrix} -12 & 5 \end{bmatrix}'$, the responses for the plant states (x_p), the control signal and the inter-event times for the PETC are shown in Fig. 5.

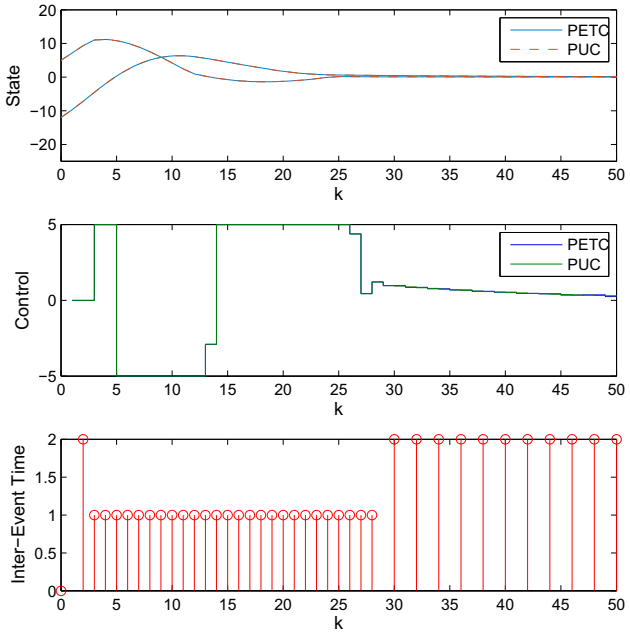

Fig. 6 Example 2: response with the PETC obtained from co-design and with the standard PUC strategy

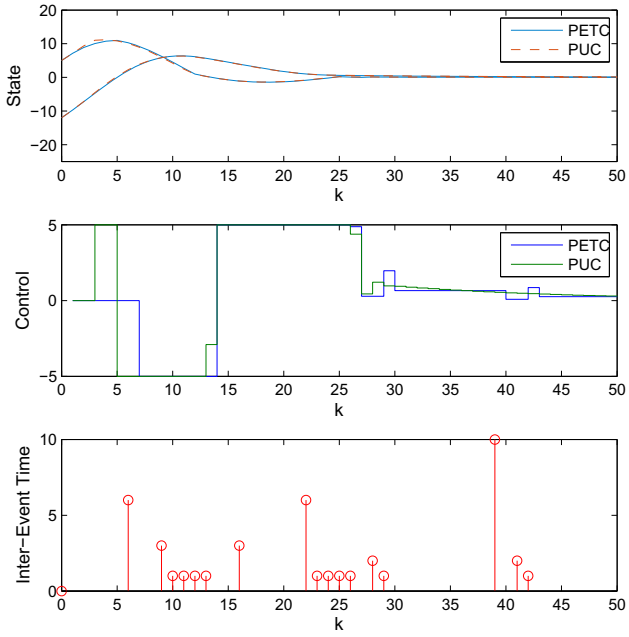

Fig. 7 Example 2: response with the PETC obtained from re-design and with the standard PUC strategy

Again, the PETC strategy has efficiently reduced the number of control updates with respect to the periodic strategy. With the PETC the control is updated 10 times versus 50 with the standard periodic updating strategy, for $0 < k \leq 50$. Note that, despite the fact that the control effectively saturates on the transient, the trajectories converge to zero, as expected.

Co-design case

For the co-design case, the same observer gain $L = [-1.16 \quad -1.91]'$ and $\alpha = 0.98$ are considered. To avoid ill conditioned solutions, a constraint $\lambda_{\max}(Q_\epsilon) < 10^4 \lambda_{min}(Q_\epsilon)$ is also considered. The optimal solution of problem (37) in this case gives:

$$Q_\delta = \begin{bmatrix} 1.48 \cdot 10^{13} & -8.439 \cdot 10^{12} \\ -8.439 \cdot 10^{12} & 1.815 \cdot 10^{13} \end{bmatrix},$$

$$Q_\epsilon = \begin{bmatrix} 1.607 \cdot 10^{-11} & 1.822 \cdot 10^{-12} & 2.841 \cdot 10^{-14} \\ 1.822 \cdot 10^{-12} & 1.564 \cdot 10^{-11} & 7.503 \cdot 10^{-14} \\ 2.841 \cdot 10^{-14} & 7.503 \cdot 10^{-14} & 9.573 \cdot 10^{-12} \end{bmatrix},$$

$$K = \begin{bmatrix} 4.176 & -11.9 \end{bmatrix}.$$

For the co-design case, with same initial conditions of the emulation case, the obtained results are shown in Fig. 6.

It can be seen that no improvement in terms of number of control updates with respect to the emulation case is obtained: 39 times in the co-design versus 10 in the emulation case. Applying therefore the re-design procedure, i.e., considering the gain K obtained in the co-design and solving (34), we have the following results:

$$Q_\delta = \begin{bmatrix} 0.8585 & -2.445 \\ -2.445 & 6.968 \end{bmatrix},$$

$$Q_\epsilon = \begin{bmatrix} 4.115 & 0.9069 & -2.096 \cdot 10^{-5} \\ 0.9069 & 3.713 & 2.76 \cdot 10^{-5} \\ -2.096 \cdot 10^{-5} & 2.76 \cdot 10^{-5} & 0.001443 \end{bmatrix}.$$

For this case, with same initial conditions as before, the response of the closed-loop system (9) is shown in Fig. 7. Now only 18 updates of the control signal are generated for $0 < k \leq 50$, which is a great improvement with respect to the initial co-design result.

5.3 Example 3: Servo System

In this example, we design a controller for a servo system consisting of a constant-field DC motor, controlled by armature voltage e_a. The controlled output is the angle of rotor θ, which is assumed to be the only measurable variable, and the control input is the voltage applied to the armature e_a, which is limited to $\pm 40V$. As usual in this type of system, the armature inductance is negligible since the electrical time constants are much smaller than the mechanical ones and the system can be represented by the following set of equations (Ogata 2009):

$$\begin{cases} R_a i_a + k_b \dot{\theta} = e_a \\ J_c \ddot{\theta} + f_c \dot{\theta} = k_a i_a \end{cases} \tag{42}$$

where i_a is the armature current and R_a, k_a, k_b, f_c and J_c are scalar system parameters.

Considering a set of system parameter values suggested in [Ogata (2009),Chapter 4] and a sampling period $T_s = 10^{-3}\,s$, a discrete-time version of the system can be cast in the form (4) with $f(u)$ being a dead-zone nonlinearity, as in Sect. 5.2, and

$$A_s = \begin{bmatrix} 1 & 0.0009962 \\ 0 & 0.9923 \end{bmatrix}, \quad B_s = B_{sf} = \begin{bmatrix} 2.771 \cdot 10^{-6} \\ 0.005534 \end{bmatrix},$$
$$C_s = \begin{bmatrix} 1 & 0 \end{bmatrix}.$$

As in this case the global stabilization could not be achieved, we consider that $f(u)$ verifies condition (2) with $J = 0.5$, provided $|u| \leq \frac{40}{1-J}$, i.e., $u \in \mathcal{S}_u = \{u \in \mathbb{R} : |0.0125u| \leq 1\}$, and a set $\mathcal{X}_0$ with $P_0 = diag(10^{10}, 10^{10}, 3, 3)$.

Emulation Case

We start by illustrating the emulation approach. For this, we consider the gain matrices $K = \begin{bmatrix} 53.14 & -5.723 \end{bmatrix}$ and $L = \begin{bmatrix} -0.09081 & -1.734 \end{bmatrix}'$, which stabilize the discrete-time closed-loop system without the event-triggering mechanism. Solving therefore the optimization problem (34) with a decay rate $\alpha = 1$, the following matrices for the triggering function are obtained:

$$Q_d = \begin{bmatrix} 481.5 & 51.85 \\ 51.85 & 5.64 \end{bmatrix}, \quad Q_e = \begin{bmatrix} 39.62 & 14.66 & 8.804 \\ 14.66 & 445.2 & 18.31 \\ 8.804 & 18.31 & 2.546 \end{bmatrix}.$$

The simulation of the resulting closed-loop system with initial conditions $x_o[0] = \begin{bmatrix} 0 & 0 \end{bmatrix}'$ and $x_p[0] = \begin{bmatrix} \frac{\pi}{6} & 0 \end{bmatrix}'$ is shown in Fig. 8. In this simulation, considering $0 < k \leq 500$, 158 events were generated. This represents a reduction of 68% in the control updating, with respect to the PUC standard strategy (which would lead to 500 control updates in the interval).

Co-design Case

Now we explore the co-design case, taking the same observer gain matrix $L = \begin{bmatrix} -0.09081 & -1.734 \end{bmatrix}'$ used in the emulation design. Solving optimization problem (37) yields

$$Q_d = \begin{bmatrix} 5.248 \cdot 10^{16} & 4.536 \cdot 10^{15} \\ 4.536 \cdot 10^{15} & 4.622 \cdot 10^{14} \end{bmatrix},$$
$$Q_e = \begin{bmatrix} 7.706 \cdot 10^{-12} & -2.6 \cdot 10^{-12} & 8.286 \cdot 10^{-15} \\ -2.6 \cdot 10^{-12} & 1.614 \cdot 10^{-11} & 1.869 \cdot 10^{-14} \\ 8.286 \cdot 10^{-15} & 1.869 \cdot 10^{-14} & 5.103 \cdot 10^{-12} \end{bmatrix},$$
$$K = \begin{bmatrix} -12.01 & -2.938 \end{bmatrix}.$$

Simulation results with the same initial conditions as in the emulation case are shown in Fig. 9. Due to the conservatism

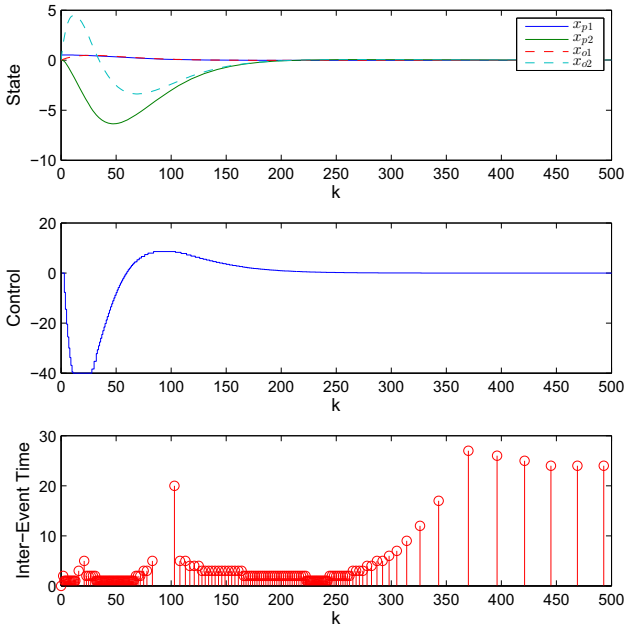

Fig. 8 Example 3– emulation response

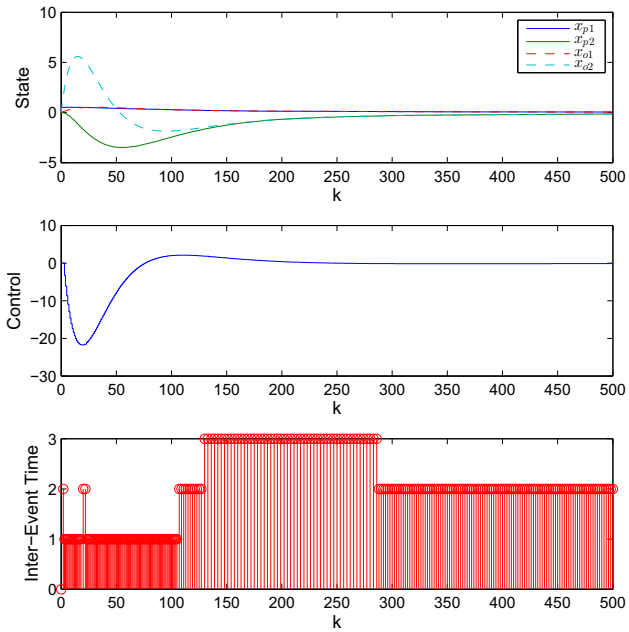

Fig. 9 Example 3—co-design response

imposed by the structured matrices used in the co-design optimization problem, the resulting event-trigger performance is poorer than in the emulation case and 274 events are generated. In the sequel, we will illustrate the re-design approach (described in Sect. 4.3) to overcome this drawback.

Re-design

Now we take the gain $K = \begin{bmatrix} -12.01 & -2.938 \end{bmatrix}$ obtained in the co-design procedure and solve the emulation case

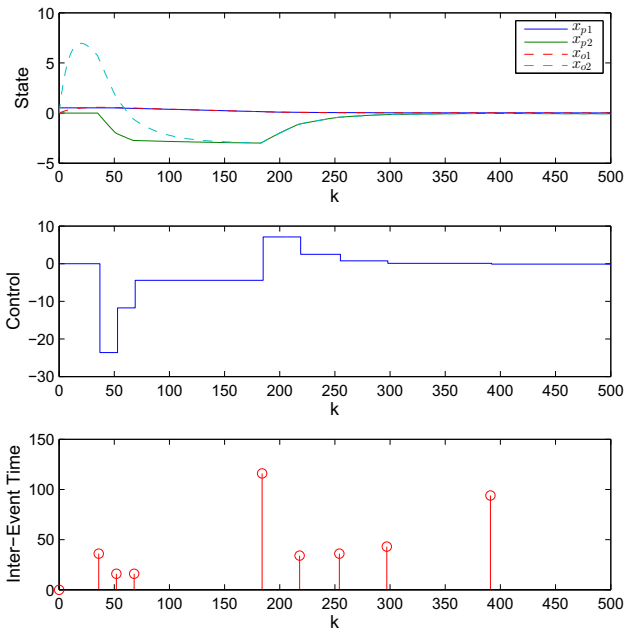

Fig. 10 Examplo 3—Re-design response

optimization problem (34), which leads to the following triggering function matrices:

$$Q_d = \begin{bmatrix} 3.279 & 0.802 \\ 0.802 & 0.1968 \end{bmatrix},$$

$$Q_e = \begin{bmatrix} 0.4908 & 0.0004328 & -4.016 \cdot 10^{-5} \\ 0.0004328 & 2.986 & -5.4 \cdot 10^{-5} \\ -4.016 \cdot 10^{-5} & -5.4 \cdot 10^{-5} & 0.001976 \end{bmatrix}.$$

Simulation results with the same initial conditions as in previous cases are shown in Fig. 10. In this case, only 9 events were generated. This illustrates how the re-design approach can be very effective.

5.4 Exemple 4: Active Suspension

For this example, we will consider the control of a quart-cart active suspension, depicted schematically in Fig. 11.

Equating the forces from the equilibrium position of x_1 and x_2, we get:

$$M_2 \frac{d^2x_2}{dt} + K_2(x_2 - x_1) + C_2\left(\frac{dx_2}{dt} - \frac{dx_1}{dt}\right) = F_c \quad (43)$$

$$M_1 \frac{d^2x_1}{dt^2} - K_2(x_2 - x_1) - C_2\left(\frac{dx_2}{dt} - \frac{dx_1}{dt}\right) - K_1(z_r - x_1) - C_1\left(\frac{dz_r}{dt} - \frac{dx_1}{dt}\right) = -F_c \quad (44)$$

where M_2 is the upper mass, which represents the car chassis, M_1 as the lower mass, which represents the car tire, K_1 and K_2 are elastic constants and C_1 and C_2 are friction constants.

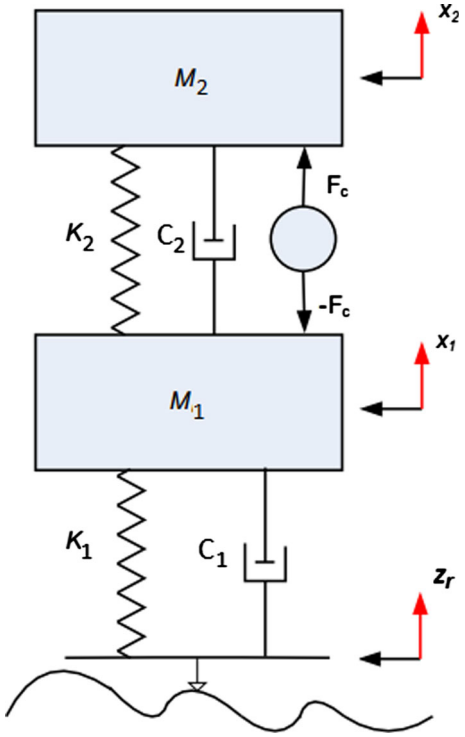

Fig. 11 Plant model

The control signal is given by the applied force F_c. x_1 and x_2 are the displacements of the tire and chassis of the car.

For control purposes, we consider the state vector and the output of the system given, respectively, by

$$x_p(t) = \begin{bmatrix} x_2 - x_1 \\ dx_2t \\ x_2 - z_r \\ dx_1t \end{bmatrix}, \qquad y(t) = x_2 - x_1. \quad (45)$$

Considering the parameters of a laboratory setup, we have that the plant can therefore be represented by the following state equation:

$$\begin{cases} \dot{x}_p(t) = \begin{bmatrix} 0 & 1 & 0 & -1 \\ -367.3 & -3.061 & 0 & 3.061 \\ 0 & 0 & 0 & 1 \\ 900 & 7.5 & -2500 & -12.5 \end{bmatrix} x_p(t) \\ \qquad\qquad + \begin{bmatrix} 0 \\ 0.408 \\ 0 \\ -1 \end{bmatrix} sat(u(t)) \\ y(t) = \begin{bmatrix} 1 & 0 & 0 & 0 \\ 0 & 0 & 1 & 0 \end{bmatrix} x(t) \end{cases} \quad (46)$$

where we considered that $F_c(t)$ is provided by a saturating actuator with saturation level of ± 20 V. Considering the dead-zone function $f(u) = sat(u) - u$, system (46) can be re-

written in the form (4), while satisfying the condition (2) with $J = 0.9$ regionally for $u \in \mathcal{S}_u = \{u \in \mathbb{R} : |0.005u| \leq 1\}$. Furthermore, this change implies $B_{sf} = B_s$. Therefore, considering a sampling period $T_s = 10^{-3}$ s, the discrete-time system (4) is obtained with

$$A_s = \begin{bmatrix} 0.9994 & 0.0009945 & 0.001243 & -0.0009916 \\ -0.3653 & 0.9968 & -0.003958 & 0.003218 \\ 0.0004475 & 3.879 \cdot 10^{-6} & 0.9988 & 0.0009932 \\ 0.8925 & 0.007885 & -2.483 & 0.9859 \end{bmatrix},$$

$$B_s = \begin{bmatrix} 7.005 \cdot 10^{-7} \\ 0.0004058 \\ -4.973 \cdot 10^{-7} \\ -0.0009916 \end{bmatrix}, \quad C_s = \begin{bmatrix} 1 & 0 & 0 & 0 \\ 0 & 0 & 1 & 0 \end{bmatrix}.$$

It is important to note that such a system is stable, but with a very oscillatory response, i.e., its poles are located in $0.9914 \pm 0.0583i$ and $0.999 \pm 0.0162i$.

Consider the emulation problem with the control gain $K = \begin{bmatrix} -2820 & 378 & -5980 & -36 \end{bmatrix}$ and the observer gain $L = \begin{bmatrix} -0.5208 & -131 & -3 & -39 \end{bmatrix}'$ and $\mathcal{X}_0$ as defined in (33), with $P_0 = \begin{bmatrix} P_{01} & 0 \\ 0 & P_{02} \end{bmatrix}$, where $P_{01} = diag(10^5,\ 10^5,\ 10^5,\ 10^5)$ and

$$P_{02} = \begin{bmatrix} 1 \cdot 10^5 & 0 & 0 & 0 \\ 0 & 2000 & 2.132 \cdot 10^{-14} & 0 \\ 0 & -2.22 \cdot 10^{-14} & 2000 & 7.806 \cdot 10^{-18} \\ 0 & 4.441 \cdot 10^{-16} & -9.454 \cdot 10^{-17} & 2000 \end{bmatrix}.$$

Applying the optimization problem (34) for the regional case, with a decay rate $\alpha = 1$, leads to the following matrices for the triggering function (11):

$$Q_\delta = \begin{bmatrix} 51.52 & 6.877 & -108.7 & -0.6529 \\ 6.877 & 1.206 & -14.58 & -0.08764 \\ -108.7 & -14.58 & 230.7 & 1.385 \\ -0.6529 & -0.08764 & 1.385 & 0.2912 \end{bmatrix},$$

$$Q_\epsilon = \begin{bmatrix} 3.588 & -2.608 & -0.3562 & -1.285 & 0.2576 & 0.37 \\ -2.608 & 88.38 & 0.7257 & -15.29 & 0.8049 & -0.8064 \\ -0.3562 & 0.7257 & 2.473 & 0.3717 & -0.1501 & -0.0005431 \\ -1.285 & -15.29 & 0.3717 & 188.7 & 0.1195 & -0.8735 \\ 0.2576 & 0.8049 & -0.1501 & 0.1195 & 0.2705 & 0.262 \\ 0.37 & -0.8064 & -0.0005431 & -0.8735 & 0.262 & 0.3547 \end{bmatrix}.$$

The simulation of the closed-loop system comparing the designed PETC and the standard PUC strategy, considering $x_o[0] = \begin{bmatrix} 0 & 0 & 0 & 0 \end{bmatrix}'$ and $x_p[0] = \begin{bmatrix} -0.012 & 0.1 & -0.001 & 0.7 \end{bmatrix}'$, results in the responses shown in Fig. 12.

As in the previous examples, the PETC strategy has efficiently reduced the number of control updates with respect to the standard periodic strategy. With the PETC the control signal is updated 23 times versus 250 with the periodic strategy, for $0 < k \leq 250$. Note that, despite the fact the control effectively saturates on the transient, the trajectories converge to zero, as expected.

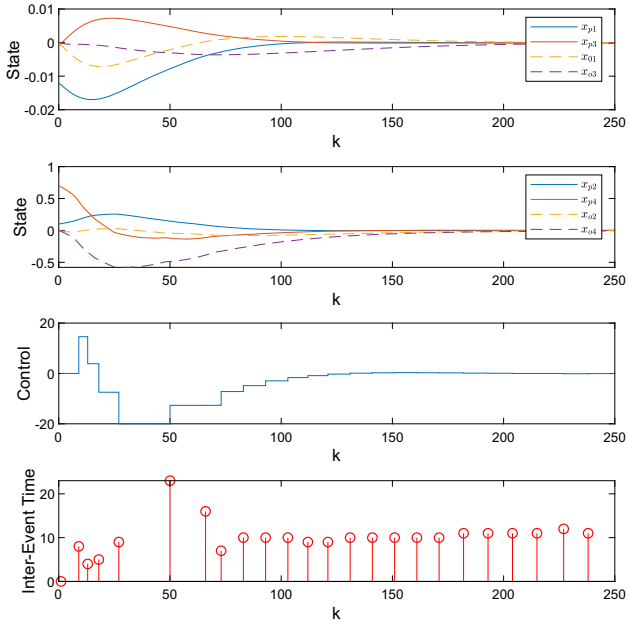

Fig. 12 Example 4: response for the emulation case

6 Conclusions

In this work, we proposed a methodology to design observer-based periodic event-triggered controllers for linear plants subject to input cone-bounded nonlinearities. The emulation, co-design and re-design cases for regional and global stabilization were addressed. The proposed triggering function uses only available information, obtained from the output and from an observer that estimates the plant state. The methodology is based on LMI conditions that ensure the stability of the system and can be cast into convex optimization problems aiming at reducing the number of control signal updates with respect to a standard periodic (time-triggered) digital implementation of the control law. The efficiency of this method is illustrated through some numerical examples. In these examples, a sensible reduction in the control updates with respect to the periodic implementation was achieved.

Funding Funding was provided by Conselho Nacional de Desenvolvimento Científico e Tecnológico, Brazil (grants PQ-305979/2019-9, Univ-42299/2016-0 and IC scholarship) and Instituto Federal de Educação, Ciência e Tecnologia Sul-rio-grandense, Brazil (Project PD00190519/011).

Compliance with Ethical Standards

Conflict of interest The authors declare that they have no conflict of interest.

References

Abdelrahim, M., Postoyan, R., Daafouz, J., & Nešić, D. (2016). Stabilization of nonlinear systems using event-triggered output feedback controllers. *IEEE Transactions on Automatic Control*, *61*(9), 2682–2687.

Aranda-Escolástico, E., Abdelrahim, M., Guinaldo, M., Dormido, S., Heemels, W. P. M. H. (2017). Design of periodic event-triggered control for polynomial systems: A delay system approach. IFAC-PapersOnLine 50(1):7887–7892, 20th IFAC World Congress

Borgers, D. P., Postoyan, R., Anta, A., Tabuada, P., Nšić, D., & Heemels, W. P. M. H. (2018). Periodic event-triggered control of nonlinear systems using overapproximation techniques. *Automatica*, *94*, 81–87.

Borgers, D. P., Dolk, V. S., & Heemels, W. P. M. H. (2017). Dynamic periodic event-triggered control for linear systems. In *Proceedings of the 20th International Conference on Hybrid Systems: Computation and Control, New York, NY, HSCC '17*, pp. 179–186

Braga, M. F., Morais, C. F., Tognetti, E. S., Oliveira, R. C., & Peres, P. L. (2015). Discretization and event triggered digital output feedback control of lpv systems. *Systems & Control Letters*, *86*, 54–65.

Campos, G. C., Gomes da Silva Jr, J. M., Tarbouriech, S., & Pereira, C. E. (2018). Stabilisation of discrete-time systems with finite-level uniform and logarithmic quantisers. *IET Control Theory Applications*, *12*(8), 1125–1132.

Chen, X., & Hao, F. (2015). Periodic event-triggered state-feedback and output-feedback control for linear systems. *International Journal of Control, Automation and Systems*, *13*(4), 779–787.

Cuenca, A., Antunes, D. J., Castillo, A., García, P., Khashooei, B. A., & Heemels, W. P. M. H. (2019). Periodic event-triggered sampling and dual-rate control for a wireless networked control system with applications to uavs. *IEEE Transactions on Industrial Electronics*, *66*(4), 3157–3166.

Eqtami, A., Dimarogonas, D. V., & Kyriakopoulos, K. J. (2010). Event-triggered control for discrete-time systems. In *Proceedings of the 2010 American control conference*, pp. 4719–4724

Gomes da Silva Jr, J. M., & Tarbouriech, S. (2005). Antiwindup design with guaranteed regions of stability: an LMI-based approach. *IEEE Transactions on Automatic Control*, *50*(1), 106–111.

Groff, L. B., Moreira, L. G., Gomes da Silva Jr, J. M., & Sbarbaro, D. (2016). Observer-based event-triggered control: A discrete-time approach. In *Proceedings of the American control conference, Boston*, pp. 4245–4250

Heemels, W. P. M. H., Johansson, K. H., & Tabuada, P. (2012). An introduction to event-triggered and self-triggered control. In *Proceedings of the IEEE conference on decision and control, Maui*, pp. 3270–3285

Heemels, W. P. M. H., Donkers, M. C. F., & Teel, A. R. (2013). Periodic event-triggered control for linear systems. *IEEE Transactions on Automatic Control*, *58*(4), 847–861.

Hespanha, J. P., Naghshtabrizi, P., & Xu, Y. (2007). A survey of recent results in networked control systems. *Proceedings of the IEEE*, *95*(1), 138–162.

Hu, S., Yue, D., Yin, X., Xie, X., & Ma, Y. (2016). Adaptive event-triggered control for nonlinear discrete-time systems. *International Journal of Robust and Nonlinear Control*, *26*(18), 4104–4125.

Jia, X. C., Chi, X. B., Han, Q. L., & Zheng, N. N. (2014). Event-triggered fuzzy H_∞ control for a class of nonlinear networked control systems using the deviation bounds of asynchronous normalized membership functions. *Information Sciences*, *259*, 100–117.

Linsenmayer, S., Dimarogonas, D. V., & Allgöwer, F. (2019). Periodic event-triggered control for networked control systems based on non-monotonic Lyapunov functions. *Automatica*, *106*, 35–46.

Liu, D., & Yang, G. H. (2019). Dynamic event-triggered control for linear time-invariant systems with $\mathcal{L}_2$-gain performance. *International Journal of Robust and Nonlinear Control*, *29*(2), 507–518.

Liu, D., Yang, G., & Er, M. J. (2020). Event-triggered control for T-S fuzzy systems under asynchronous network communications. *IEEE Transactions on Fuzzy Systems*, *28*(2), 390–399.

Moreira, L. G., Groff, L. B., & Gomes da Silva Jr, J. M. (2016). Event-triggered state-feedback control for continuous-time plants subject to input saturation. *Journal of Control, Automation and Electrical Systems*, *27*(5), 473–484.

Moreira, L. G., Tarbouriech, S., Seuret, A., & Gomes da Silva Jr, J. M. (2019). Observer-based event-triggered control in the presence of cone-bounded nonlinear inputs. *Nonlinear Analysis: Hybrid Systems*, *33*, 17–32.

Ogata, K. (2009). Engenharia de Controle Moderno, 4th edn. Pearson

Oliveira, T. G., Palhares, R. M., Campos, V. C. S., Queiroz, P. S., & Gonçalves, E. N. (2017). Improved Takagi-Sugeno fuzzy output tracking control for nonlinear networked control systems. *Journal of the Franklin Institute*, *354*(16), 7280–7305.

Peng, C., Han, Q. L., & Yue, D. (2013). To transmit or not to transmit: A discrete event-triggered communication scheme for networked Takagi-Sugeno fuzzy systems. *IEEE Transactions on Fuzzy Systems*, *21*(1), 164–170.

Postoyan, R., Anta, A., Heemels, W. P. M. H., Tabuada, & P., Nešić, D. (2013). Periodic event-triggered control for nonlinear systems. In *Proceedings of the IEEE conference on decision and control* (pp. 7397–7402). Florence

Qi, Y., Xu, X., Lu, S., & Yu, Y. (2020). A waiting time based discrete event-triggered control for networked switched systems with actuator saturation. *Nonlinear Analysis: Hybrid Systems, 37*

Selivanov, A., & Fridman, E. (2016). Event-triggered H_∞ control: A switching approach. *IEEE Transactions on Automatic Control*, *61*(10), 3221–3226.

Tabuada, P. (2007). Event-triggered real-time scheduling of stabilizing control tasks. *IEEE Transactions on Automatic Control*, *52*(9), 1680–1685.

Wang, W., Postoyan, R., Nešić, D., & Heemels, W. P. M. H. (2018). Periodic event-triggered output feedback control of nonlinear systems. In *Proceedings of the IEEE conference on decision and control (CDC)* (pp. 957–962).

Wang, W., Postoyan, R., Nešić, D., & Heemels, W. P. M. H. (2020). Periodic event-triggered control for nonlinear networked control systems. *IEEE Transactions on Automatic Control*, *65*(2), 620–635.

Yan, S., Shen, M., Nguang, S. K., Zhang, G., & Zhang, L. (2019). A distributed delay method for event-triggered control of T-S fuzzy networked systems with transmission delay. *IEEE Transactions on Fuzzy Systems*, *27*(10), 1963–1973.

Yang, J., Sun, J., Zheng, W. X., & Li, S. (2018). Periodic event-triggered robust output feedback control for nonlinear uncertain systems with time-varying disturbance. *Automatica*, *94*, 324–333.

Yue, D., Tian, E., & Han, Q. L. (2013). A delay system method for designing event-triggered controllers of networked control systems. *IEEE Transactions on Automatic Control*, *58*(2), 475–481.

Zhang, D., Han, Q. L., & Jia, X. (2015). Network-based output tracking control for T-S fuzzy systems using an event-triggered communication scheme. *Fuzzy Sets and Systems*, *273*, 26–48.